

[1]

GLOBAL RIVER RUNOFF CALCULATED FROM A GLOBAL ATMOSPHERIC GENERAL CIRCULATION MODEL

GARY L. RUSSELL and JAMES R. MILLER

¹*NASA/Goddard Space Flight Center, Institute for Space Studies, 2880 Broadway, New York, NY 10025 (U.S.A.)*

²*Department of Meteorology and Physical Oceanography, Cook College, Rutgers University, New Brunswick, NJ 08903 (U.S.A.)*

(Received June 23, 1989; accepted after revision October 24, 1989)

ABSTRACT

Russell, G.L. and Miller, J.R., 1990. Global river runoff calculated from a global atmospheric general circulation model. *J. Hydrol.*, 117: 241-254.

The purpose of this paper is to show that an atmospheric general circulation model (GCM) can be used to calculate runoff for the world's major rivers, that river runoff provides an important diagnostic for climate modelers, and that the model runoff provides useful information for hydrologists. The global atmospheric model of Hansen et al. has been used to calculate the annual river runoff for the world's major rivers. The model has a horizontal resolution of $4^\circ \times 5^\circ$, but the runoff from each grid box within a particular river's drainage basin is summed on a resolution of $2^\circ \times 2.5^\circ$ to obtain the runoff at the river mouth. The mean annual runoff is calculated and compared with observations for 33 of the world's largest rivers. The runoff depends on the model's precipitation and parameterizations of groundwater storage and evapotranspiration, which are affected by soil type and vegetation.

INTRODUCTION

The global hydrologic cycle is one of the principal components of our climate system. Across the global air-sea interface there is a net flux of water out of the ocean because evaporation exceeds precipitation. Over land, evaporation is less than precipitation. The long-term global water budgets for both continents and oceans are balanced by the continental runoff of water back to the ocean. The distribution of global runoff has been discussed in several papers (Baumgartner and Reichel, 1975; Korzoun et al., 1977; Milliman and Meade, 1983).

Atmospheric general circulation models (GCM) have been used to simulate the present climate. In the past few years, global climate modelers have begun to examine the effects of more complex parameterizations of land-atmosphere-biosphere interactions. The biosphere atmosphere transfer scheme (BATS) described in Dickinson (1984), Dickinson et al. (1986), and Wilson et al. (1987) and the simple biosphere (SiB) of Sellers et al. (1986) provide a model

framework for a more accurate representation of surface processes in GCM, particularly the interactions with vegetation and vegetation canopies. Such studies are needed if we are fully to understand the physical processes that affect the global hydrologic cycle.

An important component of the Earth's hydrologic cycle is river runoff. The world's 20 largest rivers account for $\sim 40\%$ of the total continental runoff (Baumgartner and Reichel, 1975). The river runoff for a particular drainage basin depends on the precipitation and evaporation budgets within the basin and on the ability of the ground to store water, which depends on the soil type and the vegetative cover. Flow rates depend on the topography. The comparison of model-generated river runoff with observations provides a useful diagnostic for climate modelers to obtain a better understanding of the parameterizations which affect the hydrologic cycle in their models.

An important reason for hydrologists to study model-generated river runoff is to understand and to predict future changes in river runoff that may accompany global climatic changes. Since the prediction of future changes depends on some type of model, it is essential for hydrologists and climate modelers to develop the best possible surface parameterizations that affect model-generated river runoff.

The primary purpose of this paper is to demonstrate that the calculation of river runoff in an atmospheric GCM provides a useful diagnostic for climate modelers and a useful tool for hydrologists. To accomplish this, we use the runoff from each grid box of the global atmospheric model of Hansen et al. (1983) to calculate the model-generated runoff from the world's rivers which have a mean annual discharge greater than $100 \text{ km}^3 \text{ year}^{-1}$ or a drainage basin area greater than $5 \times 10^5 \text{ km}^2$. The mean annual runoff for each river is calculated from a four-year model simulation and is compared with observations. The effect of the model precipitation, evaporation, and groundwater storage on the runoff is examined.

THE ATMOSPHERIC MODEL

A four-year simulation with the Climate Model II of Hansen et al. (1983) was run with a horizontal resolution of 4° latitude by 5° longitude and nine vertical layers. Arakawa's B grid scheme is used for the dynamics. The source terms include a comprehensive radiation calculation and parameterizations of condensation and surface interaction. At the surface, grid boxes are divided into land and ocean fractions.

The sea surface temperature (SST) and ocean ice distribution is specified from monthly climatologies interpolated on a daily basis. The SST is from Robinson and Bauer (1982). The ocean ice distribution is from Walsh and Johnson (1979) in the Northern Hemisphere and Alexander and Mobley (1976) in the Southern Hemisphere. The land distribution and continental topography is from a corrected version of Gates and Nelson (1975).

The runoff in each grid box depends on the precipitation, evaporation, and

water storage within the land portion of the grid box. The mean annual distribution of precipitation of the model is shown in Fig. 1a. For comparison, observations of precipitation by Shea (1986) are shown in Fig. 1b and a difference plot is shown in Fig. 1c. The evaporation ($\text{kg m}^{-2} \text{s}^{-1}$) is calculated as the product:

$$E = \beta \rho C V (q_s - q_a) \quad (1)$$

where β is a dimensionless efficiency factor for evaporation or evapotranspiration, ρ (kg m^{-3}) is the surface air density, C is a dimensionless drag coefficient that depends on stability, V (m s^{-1}) is the surface wind speed, q_s is the surface saturation specific humidity that depends on the ground temperature and the surface pressure, and q_a is the surface air specific humidity at 10 m above the surface.

The annual change in groundwater storage over a four-year run is insignificant compared with annual precipitation, evaporation and runoff. Nevertheless, the current stored groundwater directly affects both β and the runoff. Each grid box has two layers of groundwater storage. The upper layer responds immediately to evaporation and precipitation and the lower layer acts as a seasonal reservoir. There is a two-day time constant for diffusion of water between the two layers, except during the growing season when the upward diffusion occurs instantly over vegetated areas. The water field capacities of the two layers depend on the vegetation characteristics of each grid box and are given in Table 1 (from Hansen et al., 1983). The choice of vegetation types is described more fully in Matthews (1983).

If the soil is unsaturated, runoff, R ($\text{kg m}^{-2} \text{s}^{-1}$) is calculated as:

$$R = \frac{1}{2} P W_1 \quad (2)$$

where P ($\text{kg m}^{-2} \text{s}^{-1}$) is the precipitation and W_1 is the ratio of water in the first layer divided by the water field capacity. The factor β in eqn. (1) is equal to W_1 unless the ground is snow covered in which case $\beta = 1$. For saturated soil $R = P$.

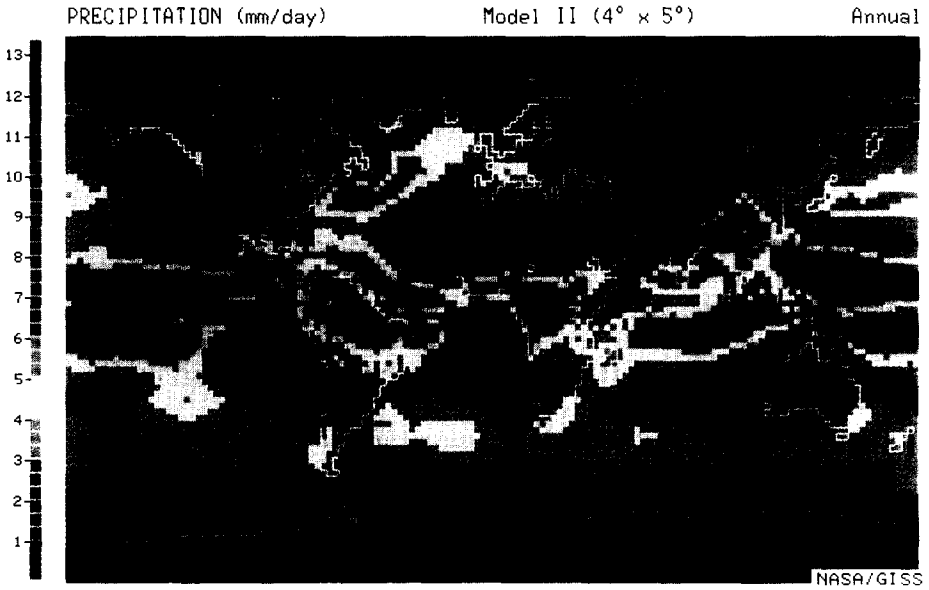
CALCULATION OF RIVER RUNOFF

The drainage basins for the rivers in this study were defined on a horizontal resolution of $2^\circ \times 2.5^\circ$ and were extracted from Korzoun et al. (1977) and the

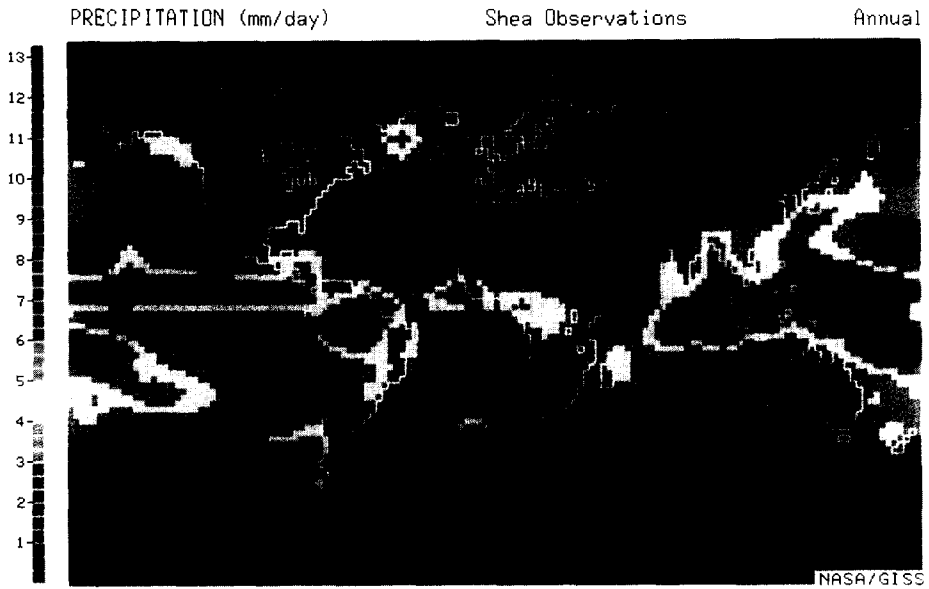
TABLE 1

Water field capacity (kg m^{-2}) as a function of vegetation characteristics in Model II.

Layer	Desert	Tundra	Grass	Shrub	Woodland	Deciduous	Evergreen	Rainforest
1	10	30	30	30	30	30	30	200
2	10	200	200	300	300	450	450	450



(a)



(b)

Fig. 1. Mean annual distribution of precipitation from (a) the atmospheric model and (b) the observed data of Shea (1986). The model precipitation minus the observed precipitation is given in (c).

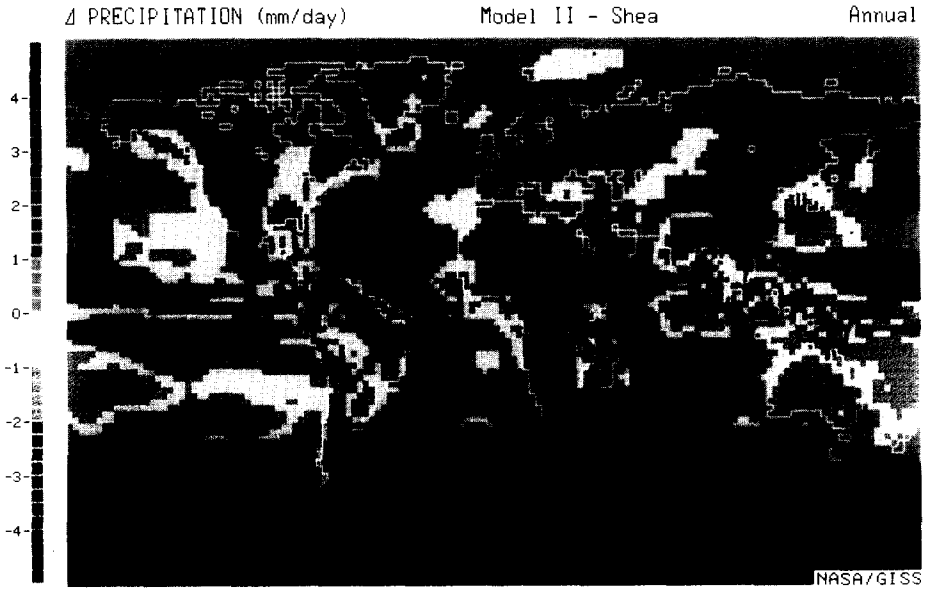


Fig. 1(c).

Major River Drainage Basins

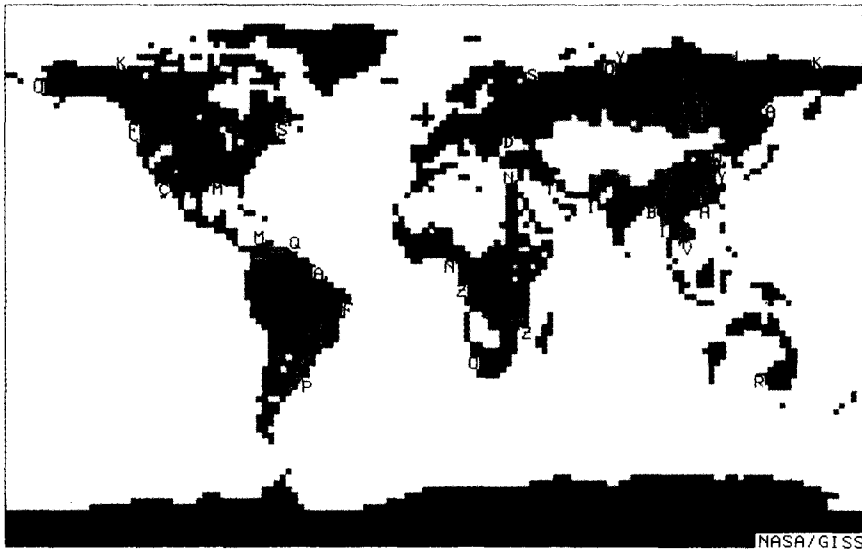


Fig. 2. Drainage basins of the rivers in this study. The letter located at the mouth of each river can be used to identify the river according to the key in Table 2. The largest river in each continent is shown in blue, other rivers with runoff $> 200 \text{ km}^3 \text{ year}^{-1}$ are shown in green and orange, and interior drainage basins are shown in yellow. Some of the identifying letters are used more than once.

Times Atlas of the World (1967). The criteria for selecting a river were an observed mean annual runoff exceeding $100 \text{ km}^3 \text{ year}^{-1}$ or drainage basin exceeding $5 \times 10^5 \text{ km}^2$ in area according to the list of rivers in Milliman and Meade (1983).

The rivers considered in this study and their drainage basin areas are listed in Table 2. Model areas are calculated by summing the areas of the $2^\circ \times 2.5^\circ$

TABLE 2

Model and observed drainage basin areas (10^{10} m^2), annual runoff ($\text{km}^3 \text{ year}^{-1}$), and annual precipitation ($\text{km}^3 \text{ year}^{-1}$) for the world's major rivers

	River	Area		Runoff		Precipitation	
		Model	Obs. ^a	Model	Obs. ^a	Model	Obs. ^b
A	Amazon	611	615	2332	6300	12267	11639
B	Brahma-Ganges	155	148	1229	971	1874	1794
C	Columbia	69	67	303	251	754	438
D	Danube	85	81	298	206	996	596
F	Fraser	24	22	150	112	289	203
H	Hsi Chiang	45	44	400	302	942	647
I	Irrawady	40	43	769	428	1345	771
K	McKenzie	169	181	562	306	1176	654
L	Lena	231	250	544	514	1414	770
M	Mississippi	327	327	517	580	2645	2439
N	Niger	121	121	351	192	1922	1217
O	Ob	266	250	504	385	1250	1117
P	LaPlata	286	283	404	470	2941	3297
Q	Orinoco	111	99	474	1100	2173	1720
S	St. Lawrence	117	103	462	447	1206	1033
T	Tigris-Euphrates	100	105	79	46	499	396
U	Yukon	88	84	492	195	780	385
V	Mekong	82	79	712	470	1997	1126
W	Yellow	113	74	515	49	1407	547
Y	Yangtze	197	194	1304	900	3442	1976
Z	Congo	382	382	2165	1250	8829	5596
A	Amur	190	185	316	325	1369	939
C	Colorado	65	64	83	20	417	165
F	San Francisco	66	64	210	97	1155	898
I	Indus	95	97	300	238	654	521
K	Kolyma	62	64	338	71	470	162
M	Magdalena	24	24	314	237	863	380
N	Nile	282	296	586	83	3509	1915
O	Orange	104	106	123	11	972	414
R	Murray	110	106	117	22	727	596
S	Severnay Dvina	33	35	117	106	224	168
Y	Yenesei	267	258	501	560	1484	989
Z	Zambesi	126	120	253	223	1589	1275

^aFrom Milliman and Meade (1983).

^bFrom Shea (1986); accumulated over the model's drainage basin.

grid boxes that lie in the appropriate drainage basins. Observed areas and runoff are from Milliman and Meade (1983).

Each of the GCM $4^\circ \times 5^\circ$ grid boxes overlies four $2^\circ \times 2.5^\circ$ grid boxes. The GCM mean annual runoff from each grid box is distributed into the $2^\circ \times 2.5^\circ$ land grid boxes. The GCM mean annual precipitation is distributed into all $2^\circ \times 2.5^\circ$ grid boxes regardless of surface type. For the model data in Table 2, the mean annual runoff or precipitation of a river's drainage basin is the summation of the runoff or precipitation from each $2^\circ \times 2.5^\circ$ grid box within the basin. Observed precipitation (Shea, 1986) is summed over the same grid boxes. In the GCM, runoff is calculated but then disappears and is not used in subsequent calculations related to the hydrologic cycle.

The runoff and precipitation in Table 2 are given in annual water mass for each river basin. In Table 3, they are given per unit area. The model runoff and precipitation and the observed precipitation from Table 2 are divided by the model drainage area, whereas the observed runoff is divided by the observed area. The evaporation is calculated as precipitation minus runoff.

The drainage basins of the rivers are shown in Fig. 2. White areas are ocean grid boxes on the $2^\circ \times 2.5^\circ$ resolution. Black areas drain to the ocean but are not included in any of the river basins in this study. The rivers with the largest discharges on each continent are shown in blue. Yellow areas are interior drainage basins that do not reach the ocean. The letter at the mouth of each river identifies the rivers according to the key in Table 2. Some letters are used more than once.

One problem associated with the model grid resolution is that a particular grid box may contain only a portion of a river drainage basin. We have accounted for this somewhat by dividing the model's grid boxes into four $2^\circ \times 2.5^\circ$ boxes for the runoff calculations. If a particular grid box is assigned to a river's drainage basin, all the continental runoff in that box is assigned to the river flow even though the actual drainage basin does not cover the whole grid box. Even with this finer resolution there are some rivers for which the drainage basin does not extend far enough because grid boxes closer to the mouth contain too much area. This problem is greatest for the smaller and narrower drainage basins, particularly in mountainous regions in Asia.

COMPARISON WITH OBSERVATIONS

The drainage basins in Fig. 2 were used to calculate the mean annual river runoff from the model. Figure 3 shows the mean annual runoff for the five largest rivers and comparison with the observed values of Milliman and Meade (1983). The model-generated runoff from the Amazon and Orinoco Rivers in South America is less than half the observed values. However, the model runoff for the Congo is about twice the observed value. The model overpredicts the runoff for the Brahmaputra–Ganges and the Yangtze Rivers by about 30%.

Although the five largest rivers have observed mean annual runoff of about $1000 \text{ km}^3 \text{ year}^{-1}$, except for the Amazon which is six times larger, most of the

TABLE 3

Model and observed runoff, precipitation and evaporation per unit area (m year^{-1}) for the world's major rivers.

	River	Runoff		Precipitation		Evaporation ^c	
		Model	Obs. ^a	Model	Obs. ^b	Model	Obs.
A	Amazon	0.38	1.02	2.01	1.90	1.62	0.88
B	Brahma-Ganges	0.80	0.66	1.21	1.16	0.42	0.50
C	Columbia	0.44	0.37	1.09	0.63	0.65	0.26
D	Danube	0.35	0.25	1.17	0.70	0.82	0.44
F	Fraser	0.64	0.51	1.23	0.86	0.59	0.35
H	Hsi Chiang	0.88	0.69	2.08	1.43	1.20	0.74
I	Irrawady	1.92	1.00	3.36	1.92	1.44	0.93
K	McKenzie	0.33	0.17	0.70	0.39	0.36	0.22
L	Lena	0.24	0.21	0.61	0.33	0.38	0.13
M	Mississippi	0.16	0.18	0.81	0.75	0.65	0.57
N	Niger	0.29	0.16	1.59	1.00	1.30	0.85
O	Ob	0.19	0.15	0.47	0.42	0.28	0.27
P	LaPlata	0.14	0.17	1.03	1.15	0.89	0.99
Q	Orinoco	0.43	1.11	1.96	1.55	1.53	0.44
S	St. Lawrence	0.40	0.43	1.03	0.88	0.64	0.45
T	Tigris-Euphrates	0.08	0.04	0.50	0.39	0.42	0.35
U	Yukon	0.56	0.23	0.88	0.44	0.32	0.20
V	Mekong	0.87	0.59	2.45	1.38	1.57	0.78
W	Yellow	0.45	0.07	1.24	0.48	0.79	0.42
Y	Yangtze	0.66	0.46	1.75	1.00	1.08	0.54
Z	Congo	0.57	0.33	2.31	1.47	1.75	1.14
A	Amur	0.17	0.18	0.72	0.50	0.56	0.32
C	Colorado	0.13	0.03	0.64	0.25	0.52	0.22
F	San Francisco	0.32	0.15	1.75	1.36	1.43	1.21
I	Indus	0.32	0.25	0.69	0.55	0.37	0.30
K	Kolyma	0.55	0.11	0.76	0.26	0.22	0.15
M	Magdalena	1.28	0.99	3.52	1.55	2.24	0.56
N	Nile	0.21	0.03	1.24	0.68	1.04	0.65
O	Orange	0.12	0.01	0.93	0.40	0.82	0.39
R	Murray	0.11	0.02	0.66	0.54	0.55	0.52
S	Severnay Dvina	0.35	0.30	0.68	0.51	0.32	0.21
Y	Yenesei	0.19	0.22	0.55	0.37	0.37	0.15
Z	Zambesi	0.20	0.19	1.26	1.01	1.06	0.83

^aFrom Milliman and Meade (1983).

^bFrom Shea (1986); accumulated over the model's drainage basin.

^cPrecipitation minus runoff.

other major river drainage basins have mean annual runoff between 200 and $600 \text{ km}^3 \text{ year}^{-1}$. Figure 4 shows the model and observed runoff for these other major rivers. The model runoff is within $\sim 20\%$ of the observed runoff for half of the 16 rivers shown in Fig. 4, and within 30–40% for the rest except for the Mekong, Irrawaddy and McKenzie, which are all overpredicted by the model.

Runoff was also calculated for other rivers with relatively large drainage basins (areas $> 5 \times 10^5 \text{ km}^2$) but lower runoff. These are shown in Fig. 5. The

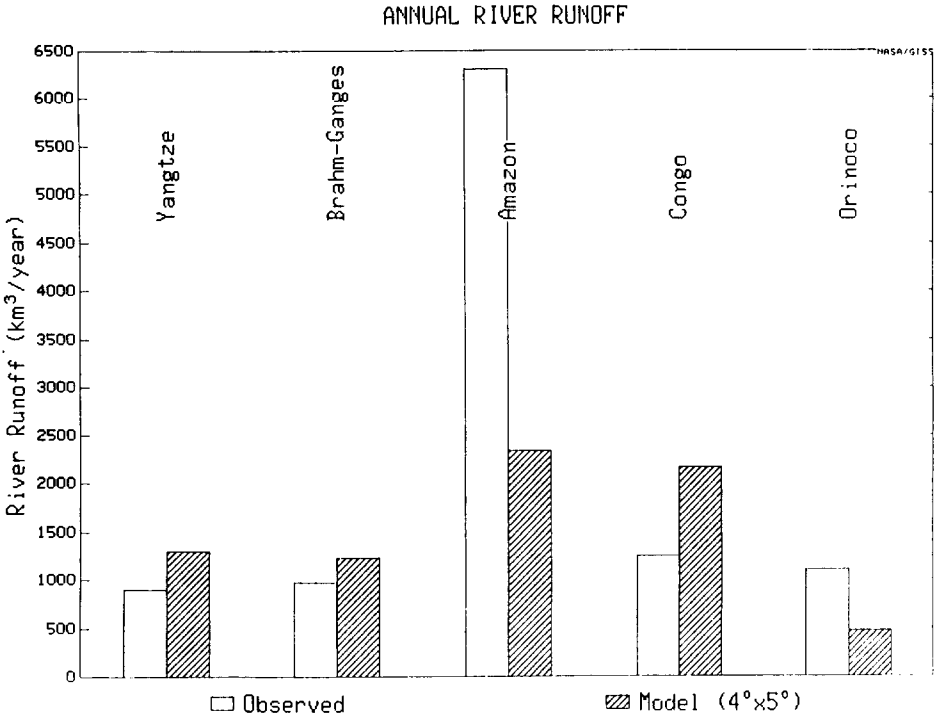


Fig. 3. Mean annual runoff for the world's five largest rivers. Comparison between model runoff and the observed runoff of Milliman and Meade (1983).

Fraser River is also included because its runoff is $> 100 \text{ km}^3 \text{ year}^{-1}$. The model runoff is overpredicted for all of these rivers, and is more than seven times too large for the Nile and Yellow Rivers. Many of the river basins in this figure have mean annual observed precipitation $< 0.5 \text{ m year}^{-1}$ (Table 3) and the model overpredicts the runoff in all of these basins. The precipitation field over continents is one of the major deficiencies of the model since the model overpredicts the mean annual precipitation over continents by $\sim 25\%$. For the runoff calculations this becomes more critical for basins with lower mean annual runoff as shown in Fig. 5.

Another problem associated with the model runoff in Fig. 5 is that the model does not allow runoff to evaporate as it moves from one grid box to another. Since many of these rivers are in dry regions, the neglect of this evaporation is likely to lead to overprediction of the runoff. As an example of water loss in the Nile River, Chan and Eagleson (1980) have shown that $\sim 60\%$ of the flow of the White Nile disappears in swamps before reaching the junction with the Blue Nile at Khartoum. If this were incorporated into the model, the predicted runoff for the Nile would be significantly reduced.

Figure 1a shows that the model precipitation in northern Asia is generally low, although Fig. 1c shows that the model precipitation is somewhat larger

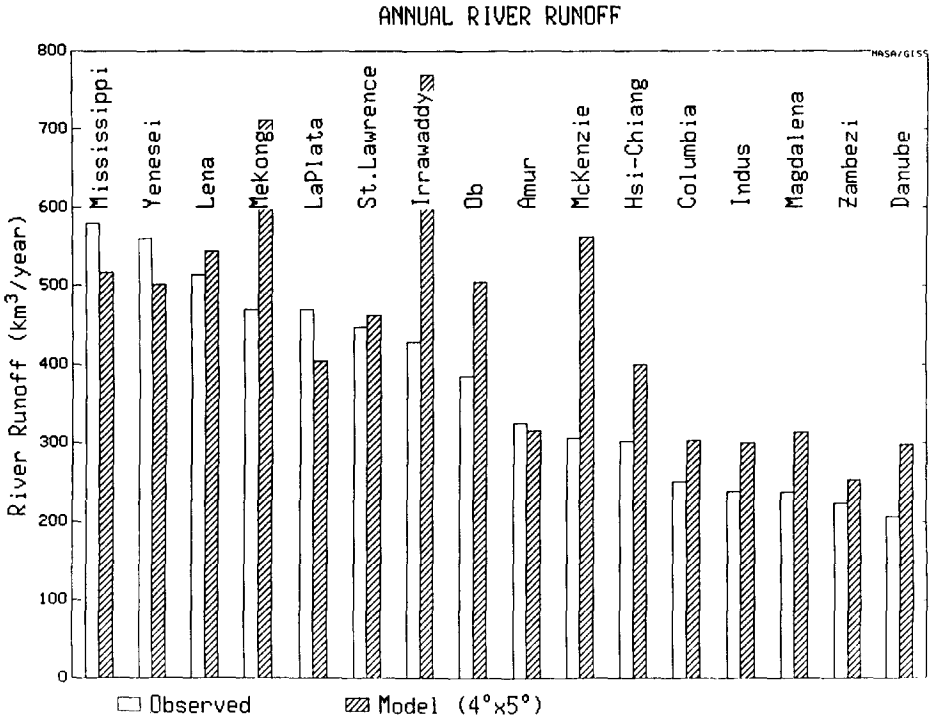


Fig. 4. Model and observed runoff for rivers with observed mean annual runoff > 200 km³ year⁻¹ that are not shown in Fig. 3. Observed runoff from Milliman and Meade (1983).

than the observations. This is an example of a case where the runoff may be modeled well even though the precipitation is too large. This indicates that there is too much evaporation, partly because of the parameterization of groundwater storage and partly because of the influence of vegetation. Although we have considered only the mean annual runoff, the seasonal variation of both precipitation and runoff should be examined further in future studies.

Although the large high latitude rivers in Asia are in good agreement with observations, that is not true of the McKenzie and Yukon Rivers in North America. The comparison of the precipitation fields in Fig. 1 shows that the model generates too much precipitation in these two river basins and that the excess model runoff is directly related to the excess precipitation. The modeled runoff and precipitation for the Mississippi and St. Lawrence Rivers are in good agreement with the observed values.

South America has two of the world's five largest rivers and the model underpredicts the runoff for both the Amazon and Orinoco Rivers by > 50%. Again it is useful to examine the precipitation field in Fig. 1 and Tables 2 and 3. The model precipitation for both basins is actually too large, which seems to

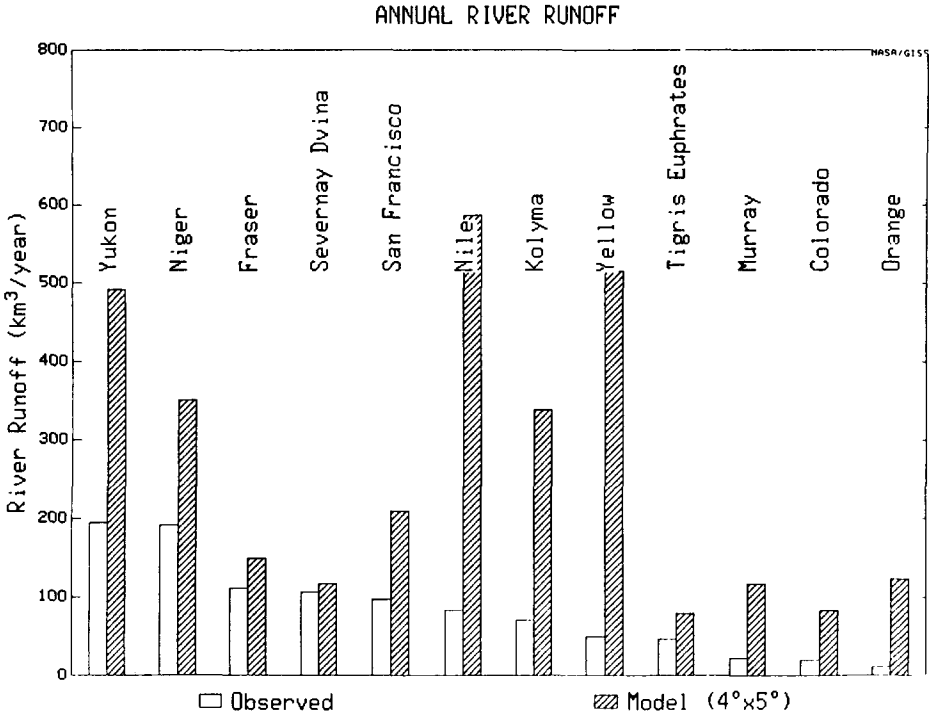


Fig. 5. Model and observed runoff for other rivers with mean annual runoff $> 100 \text{ km}^3 \text{ year}^{-1}$ or drainage basin area $> 5 \times 10^6 \text{ km}^2$. Observed runoff from Milliman and Meade (1983).

be inconsistent with our low runoff. The problem may lie in the parameterization of evapotranspiration or in the parameterization of groundwater storage.

Abramopoulos et al. (1988) have developed a new hydrology scheme to use in GCM to better model evapotranspiration and soil water movement. Dickinson and Henderson-Sellers (1988) and Henderson-Sellers et al. (1988) have shown the importance of using improved parameterizations of micrometeorological processes in the forest canopy for a better simulation of the hydrologic cycle in tropical rainforests.

If the groundwater storage capacity is too large, water will remain in the grid box to evaporate back into the atmosphere rather than leave the grid box as runoff. If the capacity were reduced, the model's runoff in the Amazon basin might improve. This could produce increased runoff and also reduce the amount of water that evaporates from the ground to be recycled as precipitation. Delworth and Manabe (1988) have discussed the significance of soil wetness parameterizations, potential evaporation and precipitation on the hydrologic balance and runoff in atmospheric models.

In southeast Asia, the model's high runoff in the Mekong, Yangtze and Irrawaddy Rivers is primarily owing to the model's excess rainfall as shown in

Fig. 1c. The same high runoff and precipitation occur in the model for the Congo and Niger Rivers. These results are generally consistent with our expectations that overprediction of runoff will occur in regions where the precipitation is overpredicted. However, there are also regions, notably the Amazon and Orinoco Rivers, where the runoff is much too low even though the precipitation is too large. It is essential that the model includes a good parameterization of the groundwater storage and evapotranspiration.

DISCUSSION AND SUMMARY

River runoff is an important component of the global hydrologic cycle. It depends on the precipitation, evaporation and groundwater storage within the river basin. We have shown that global atmospheric models can be used to calculate the mean annual river runoff for the world's largest rivers. For about half of the rivers with runoff $> 200 \text{ km}^3/\text{year}^{-1}$, the model runoff is within $\sim 20\%$ of the observed value. We will briefly discuss some of the limitations of the present model in predicting river runoff.

The comparison of model river runoff with observations is a good diagnostic for atmospheric models. Since the ratio of observed precipitation to observed river runoff varies from ~ 1.5 to 40, there is considerable variation in the amount of evaporation from different regions of the Earth's land surface. Because of this variability, it is difficult for a climate model to simulate river runoff accurately. In some cases, model river runoff may be accurate because of offsetting errors in precipitation and groundwater storage.

One of the most important comparisons is the model precipitation with observations. Figure 1c shows locations where the model precipitation is in best agreement with observations. By comparing the location of the river basins in Fig. 2 with the precipitation in Fig 1c, or by using Tables 2 and 3, one can find the basins in which the model's precipitation is too large, although for some of these basins the runoff agrees with observations. This indicates the importance of good parameterizations of groundwater storage and evapotranspiration. The runoff in the Amazon and Orinoco basins shows that even when the model precipitation is too large, the runoff can be too low because there is too much storage of water in the ground or too much evaporation. Hence, the primary concerns of atmospheric modelers in predicting runoff is to obtain accurate surface precipitation, evapotranspiration and groundwater storage including the effects of soil type and vegetation.

The grid resolution of the model can also affect the runoff. Although we did divide the model's $4^\circ \times 5^\circ$ grid boxes into four smaller boxes to calculate the river runoff, whenever a particular $2^\circ \times 2.5^\circ$ grid box was assigned to a river drainage basin, all the runoff in that grid box was assigned to the drainage basin. This assumption is likely to be most critical for some of the southeast Asian rivers where up to three major rivers pass through the same grid box in the Himalayan Mountains. One way to address this problem would be to refine the river drainage basins even more by assigning the appropriate percentage

of a grid box's runoff to the river drainage basin or by using a finer resolution model. Because the runoff in adjacent model grid boxes can vary by an order of magnitude or more, the resolution can significantly affect the total runoff in the drainage basin.

There are other problems with the formulation of the model's runoff. The calculated runoff during a time step is assumed to disappear into an infinite ocean. It cannot evaporate during subsequent time steps or interact with adjacent grid boxes. Future model development should allow for such interactions and should incorporate runoff rates that depend on the surface topography. This would have a particularly large effect on monthly runoff since there are lags between river runoff at the mouth of a large river system and the precipitation near the headwaters. The seasonal variability of the model runoff should be compared with observations to determine whether the mean annual results, if predicted correctly, are the result of correctly predicting the seasonal variability.

Another reason for differences between model-generated runoff and observations is the quality of the observed data. For several rivers there is a significant difference between the observed runoff given by Milliman and Meade (1983) and that given by Baumgartner and Reichel (1975). We used the more recent reference in our study. Milliman and Meade (1983) also included information on the quality of the data used to obtain the observed runoff in different basins.

Overall, the model runoff agrees reasonably well with observations for rivers with runoff greater than $200 \text{ km}^3 \text{ year}^{-1}$, but the model overpredicts the runoff for rivers with less than $200 \text{ km}^3 \text{ year}^{-1}$. Some of the inaccuracy occurs because of poor model precipitation fields, but the model's parameterizations of groundwater storage and evapotranspiration are also suspect. New parameterizations, including the effects of both soil type and vegetation, should be investigated. In addition to being a good diagnostic for atmospheric modelers, the runoff that may occur during future climate change can also be studied with these models.

ACKNOWLEDGEMENTS

We would like to thank R. Reudy for helping to prepare the data files for this study. We would also like to thank A. Broccoli, W. Broecker, I. Fung, D. Rind, and C. Rosenzweig for helpful discussions on various aspects of the work. We are particularly grateful to B. Oppenheimer for helping to define the river basins.

REFERENCES

- Abramopoulos, F., Rosenzweig, C. and Choudhury, B. 1988. Improved ground hydrology calculations for global climate models (GCMs): Soil water movement and evapotranspiration. *J. Climate*, 1 (9): 921-941.
- Alexander, R.C. and Mobley, R.L. 1976. Monthly average sea-surface temperatures and ice-pack limits on a 1° global grid. *Mon. Weather Rev.*, 104: 143-148.

- Baumgartner, A. and Reichel, E., 1975. *The World Water Balance*. Elsevier, Amsterdam.
- Chan, S.-O. and Eagleson, P.S., 1980. Water balance studies of the Bahr El Ghazal Swamp. Rep. No. 161, Ralph M. Parsons Lab. Water Resour. Hydrodyn., MIT, Cambridge, MA.
- Delworth, T. and Manabe, S., 1988. The influence of potential evaporation on the variabilities of simulated soil wetness and climate. *J. Climate*, 1 (5): 523-547.
- Dickinson, R.E., 1984. Modeling evapotranspiration for three-dimensional global climate models. In: *Climate Processes and Climate Sensitivity*. Geophys. Monogr. 29, Maurice Ewing Ser. AGU. Washington, D.C, 5, pp. 58-72.
- Dickinson, R.E., Henderson-Sellers, A., 1988. Modelling tropical deforestation: A study of GCM land-surface parameterizations. *Q.J.R. Meteorol. Soc.*, 114: 439-462.
- Dickinson, R.E., Henderson-Sellers, A., Kennedy, P.J. and Wilson, M.F., 1986. Biosphere-atmosphere transfer scheme (BATS) for the NCAR Community Climate Model. NCAR, Boulder, CO. Tech. Note/TN-275 + STR.
- Gates, W.L., and Nelson, A.B., 1975. A new (revised) tabulation of the Scripps topography on a 1° global grid. Part I: Terrain heights. Rep. R-1276-1-APRA, Rand Corp., Santa Monica, 132 pp.
- Hansen, J., Russell, G., Rind, D., Stone, P., Lacis, A., Lebedeff, S., Reudy, R. and Travis, L., 1983. Efficient three-dimensional global models for climate studies: Models I and II. *Mon. Weather Rev.*, 111(4): 609-662.
- Henderson-Sellers, A., Dickinson, R.E. and Wilson, M.F., 1988. Tropical deforestation: Important processes for climate models. *Climatic Change*, 13: 43-67.
- Korzoun, V.I., Sokolov, A.A., Budyko, M.I., Voskresensky, K.P., Kalinin, G.P., Konoplyantsev, A.A., Korotkevich, E.S., Lvovich, M.I. (Editors), 1977. *Atlas of World Water Balance*. USSR National Committee for the International Hydrological Decade, UNESCO, Paris.
- Matthews, E., 1983. Global vegetation and land use: New high-resolution data bases for climate studies. *J. Climate Appl. Meteorol.*, 22: 474-487.
- Milliman, J.D. and Meade, R.H., 1983. World-wide delivery of river sediment to the oceans. *J. Geol.*, 91 (1): 1-21.
- Robinson, M.K. and Bauer, R.A., 1982. Sea surface temperature climatology. In: S. Auer (Editor). *NOAA Oceanographic Monthly Summary*, April.
- Sellers, P.J., Mintz, Y., Sud, Y.C. and Dalcher, A., 1986. A simple biosphere model (SiB) for use within general circulation models. *J. Atmos. Sci.*, 43 (6): 505-531.
- Shea, D., 1986. *Climatological Atlas: 1950-1979, Surface Air Temperature, Precipitation, Sea-Level Pressure and Sea-Surface Temperature (45°S-90°N)*. Nat. Center Atmos. Res./TN-269 + STR, Boulder, CO.
- Times Atlas of the World, 1967. The Times of London, John Bartholomew, Edinburgh.
- Walsh, J. and Johnson, C., 1979. An analysis of Arctic sea ice fluctuations. *J. Phys. Oceanogr.* 9: 580-591.
- Wilson, M.F., Henderson-Sellers, A., Dickinson, R.E. and Kennedy, P.J., 1987. Sensitivity of the Biosphere-Atmosphere Transfer Scheme (BATS) to the inclusion of variable soil characteristics. *J. Climate Appl. Meteorol.*, 26, 341-362.